TROPOPAUSE VARIATIONS IN THE EQUATORIAL REGION

XUELONG ZHOU

Marine Science Research Center

Stony Brook University

Stony Brook, NY 11794 USA

E-mail: xzhou@notes.cc.sunysb.edu

Stratosphere-troposphere exchange (STE) is dominated by the meridional circulation with upward motion in the tropics and downward motion in the polar regions. When tropospheric air enters the stratosphere across the tropical tropopause, it is dehydrated by cold tropopause temperatures. Thus, the tropical tropopause temperatures are essential to explain observed distribution pattern and interannual variations of stratospheric water vapor. Investigations about the tropical tropopause also provide information about the coupling between the stratosphere and troposphere in the Tropics. In this review article, the author summarized recent research on tropical tropopause.

The tropical tropopause was found to be influenced by the stratospheric quasi-biennial oscillation (QBO), the tropospheric El Niño southern oscillation (ENSO) and Madden Julian oscillation (MJO). The MJO in the tropopause temperatures (CPT-T) shows Kelvin wave features in the deep Tropics and Rossby wave features in the subtropics. The QBO in the CPT-T is mainly zonally symmetric and is associated with downward propagating temperature anomalies accompanying the QBO meridional circulation. The influence of the ENSO on the tropical tropopause shows east-west dipole and north-south dummbell features. A cooling trend of the tropical CPT-T was found. This cooling trend could not explain the observed positive trend of stratospheric water vapor if the tropical tropopause temperature were the only factor which determines stratospheric water vapor concentration. Preliminary discussion about three-dimensional structure of the tropical “cold trap” is also presented.

1. Introduction

Variations of the tropical tropopause are of interest for quantifying climate variability and for understanding mechanisms of the coupling between the stratosphere and the troposphere. Compared with other trace gases, water vapor has its superior character. It experiences phase change at the tropical tropopause. Brewer (1949) noted that the distribution of stratospheric water vapor could only be explained if there exists a meridional overturning circulation that transports water vapor upward into the stratosphere through the cold tropical tropopause with poleward and downward transport at high latitudes. Dobson (1956) pointed out that a similar circulation is required to explain the observed distribution of stratospheric ozone. To honor their works, this circulation is called the "Brewer-Dobson" circulation. It should be regarded as a Lagrangian mean circulation and can be approximated by the residual circulation of the transformed Eulerian mean equations (Dunkerton, 1978). The source of most stratospheric water vapor is methane oxidation (e.g., LeTexier et al. 1988). Methane oxidation and transport effect of the "Brewer-Dobson" circulation are important in determining the climatological pattern of stratospheric water vapor, with more water vapor in the upper stratosphere than in the lower stratosphere, and more in the polar stratosphere than in the tropical stratosphere. Contrary to intuition, the troposphere is a sink of stratospheric water vapor rather than a source. The crucial factor in determining stratospheric water vapor is the cold tropical tropopause temperatures. In summary, there are three factors controlling stratospheric water vapor concentration: dehydration at the tropical tropopause, methane oxidation, and transport effect of the residual circulation.

Because tropospheric air enters the stratosphere mainly through the tropical tropopause, investigations of variations and structure of the tropical tropopause are of fundamental importance for stratospheric water vapor. This paper reviews recent studies on the tropical

tropopause. There are several definitions of the tropopause, e.g. lapse rate tropopause, cold point tropopause (CPT) and transition layer tropopause etc. (Highwood and Hoskins, 1998). Different tropopause definitions were applied in literatures for different purposes. The CPT definition of tropical tropopause, the position of coldest temperature in tropical vertical temperature profile, was used by the author in studies on tropopause variations, with emphasis on the dehydration effect of the cold tropopause temperature on stratosphere water vapor.

This paper is arranged as follows. In section 2, the seasonal cycle of the tropical tropopause was presented. Intraseasonal variations of the tropical tropopause temperatures were described in section 3. In section 4, signatures of the quasi-biennial oscillation (QBO) and the El Niño and southern oscillation (ENSO) were reviewed. In section 5, the trend of the tropical tropopause temperature was discussed. A preliminary discussion about the structure of the "cold trap" is presented in section 6. The last section is the summary.

2. Seasonal Cycle of Tropical CPT Temperatures

Failure of freeze drying at the mean tropopause temperature to dehydrate the stratosphere to the observed water vapor mixing ratio led Newell and Guld-Stewart (1981) to propose the "stratospheric fountain" hypothesis. Newell and Gould-Stewart (1981) showed that sufficiently cold temperatures were frequently found over the maritime continent warm pool region in January and were also found, though less frequently, over the Indian summer monsoon region during July. They suggested that tropospheric air enters the stratosphere mostly at these preferred times and locations. This is the "stratospheric fountain" hypothesis. Atticks and Robinson (1983) were the first to look at Brewer hypothesis by examining tropical radiosondes. Frederick and Douglass (1983) extended the analysis of Newell and

Gould-Stewart using eight years of rawinsonde data from eight tropical stations. Their results are generally consistent with Newell and Gould-Stewart (1981).

Figure 1 shows the tropical CPT temperatures (CPT-T) in January and July averaged over the 15-year ECMWF reanalysis period (1973-1993). The CPT was obtained by applying cubic spline fitting to ECMWF reanalysis daily data. Comparison between the CPT calculation based on reanalysis and high resolution sounding data indicated that the ECMWF based CPT has a warm bias about 2K and the NCEP based CPT has a warm bias about 4K (Zhou 2000; Randel et al. 2000). However, the bias is almost longitudinally uniform and mainly exists in the seasonal cycle. The western Pacific, the "stratospheric foutain" area, is the coldest region in the tropics. In summer, cold CPT area extends to the region over Tibetan though the coldest region is still over the western Pacific. This is an indication of the influence of summer monsoon on the tropical tropopause. It can be seen in Figure 1 that the tropical CPT is about 4 K colder in winter than in summer (Zhou, 2000). Consistently, the CPT is higher in altitudes and lower in pressure in winter than in summer (figures not shown). This annual cycle is mainly caused by the annual variation of the extratropical wave forcing (Yulaeva et al. 1994), and is consistent with the "tape recorder" signal in stratospheric water vapor (Mote et al. 1996). However, this consistency does not mean that air parcel across the tropical CPT is dehydrated at the monthly and/or zonal mean temperatures. Generally, the monthly and/or zonal tropopause temperature is too warm to dehydrate water vapor content to the entry value of mixing ratio (Zhou et al. 2001a). Figure 1 also indicates a zonally asymmetric feature, i.e. the western Pacific is colder than other regions. This is due to zonal asymmetry in the distribution of diabatic heating (Highwood and Hoskins, 1998).

Freeze drying to the saturation mixing ratio characteristics of the exceptionally cold tropopause temperature over the western Pacific is obviously required to explain the observed low stratospheric water vapor concentration. Such dehydration would appear to require slow upwelling in this region to produce condensation and allow ice crystals to have enough time to sediment. However, wind analysis suggested that the mean vertical wind might be downward (Sherwood 2000; Gettelman et al. 2000). To resolve this paradox, Holton and Gettelman (2001) suggested a new term "cold trap" to replace the term "fountain" and proposed a mechanism model. In their model, air parcels, which may first enter the tropopause transition layer at longitudes other than the western Pacific, encounter the "cold trap" and get dehydrated due to fast zonal motion.

3. Intraseasonal Variations of the Tropical CPT Temperature

The MJO is a major component of tropical low-frequency variations. The oscillation is a result of large-scale circulation cells oriented in the equatorial plane that move eastward from the Indian Ocean to the central Pacific Ocean (Madden and Jullia 1994). The oscillation has a range of periods of about 30-60 days and is manifest in eastward-propagating complex convective regions. Zhou and Holton (2002) analyzed the influence of the MJO in the tropical tropopause temperatures, and documented the relationship between the tropical CPT and tropical convection with focus on wave patterns in the tropical tropopause temperatures induced by tropospheric convection, using daily tropical CPT derived from the ECMWF reanalyses (1979-1993).

Figure 2 show time-longitude sections of outgoing longwave radiation (shaded) and CPT-T (contoured) averaged over the latitude band 5˚S-5˚N for the period November 1992 – February 1993. This period included two strong MJO events, whose start points were labeled

by letter A and B, respectively. The left column is for the original fields, and the right column for the 25-70 day bandpassed fields. It can be seen in Figure 2a that CPT-T is colder when there is strong convection (indicated by low OLR). However, it seems that cold CPT-T appears a little earlier than low OLR at a given longitude, or cold CPT-T is to the east of small OLR at a given time from the Indian Ocean to the western Pacific. This phase lag is more obvious in the bandpassed fields (Figure 2b). Correlation analysis demonstrated that the MJO in CPT-T leads the MJO in OLR by 8-12 days, about one quarter or typical MJO period (figures not shown).

Zhou and Holton (2002) further made composites using daily CPT data during 1979-1993. Figure 3 shows composites of the 25-70 day bandpassed OLR (shaded) and CPT-T (contoured) anomalies during the period when the 25-70 day bandpassed OLR at reference points (0˚, 85˚E) and (0˚, 125˚E) are less than -30 Wm^{-2}. The Kelvin wave pattern is obvious in the deep Tropics, and there is a Rossby wave pattern in the subtropics. The maximum CPT-T anomalies lead the OLR anomalies by one quarter wavelength over both the Indian Ocean and the western Pacific. Hendon and Salby (1996) simulated the composite life cycle of the MJO using the diabatic heating that was prescribed from the anomalous OLR in the life cycle of the MJO constructed by Hendon and Salby (1994). The composites of CPT-T shown in Figure 3 show patterns, if the sign is reversed, generally similar to the temperature patterns on day 5 and day 15 shown in Figure 2 of Hendon and Salby (1996), which is for simulated tropospheric mean temperature anomalies.

Zhou and Holton (2002) also analyzed the 6-25 day variation, which is an important component of tropical intraseasonal variations (Vincent et al. 1998). The 6-25 day variation in CPT-T leads the 6-25 day variation by one quarter period, and there are indications of Kelvin wave in the deep Tropics and Rossby wave in composites like Figure 3.

Wheeler et al. (2000) found large tropopause temperature perturbations associated with equatorial waves coupled to convection. These signals lead those in OLR for the convectively coupled Kelvin and eastward and westward inertio-gravity waves and could be interpreted as a vertically propagating response excited by a moving equatorial heat source. Using radiosonde and the NCEP reanalysis data and the lapse-rate tropopause definition, Kiladis et al. (2001) showed that the MJO displays an upward- and eastward-tilting temperature structure, indicating that the tropopause temperature disturbance leads the convection.

The Kelvin wave pattern in the tropical CPT is also consistent with some sounding observations. Boehm and Verlinde (2000) used sounding data observed in the summer of 1999 at the Republic of Nauru to find that the tropical tropopause is affected by stratospheric waves with a timescale of several days and an amplitude of up to 8 K in temperature near the tropopause. These waves have been identified as Kelvin waves, which have their origin in the troposphere (Holton et al. 2001). Tsuda et al. (1994) reported Kelvin waves with periods of about 7 and 20 days observed by radiosonde in the province of East Java, Indonesia (7.57ºS, 112.68ºE) during 27 February–22 March 1990. Both 7- and 20-day Kelvin waves have relatively larger amplitudes in a shallow vertical range near the tropical tropopause and relatively smaller amplitudes in the troposphere. Temperature anomalies associated with these waves show different signs above and below 15 km, which is about 2 km below the CPT.

4. Interannual variations of the Tropical CPT Temperatures

The stratospheric QBO and the tropospheric ENSO are two of the dominant interannual variations in the Tropics. Some features and the influence of the QBO and ENSO on the tropical tropopause were reported before the year 2000, limited to sparse tropical stations

(e.g., Reid and Gage 1981, 1985, 1996; Frederick and Douglass 1983; Gage and Reid 1987). Only recently were features of tropopause over the entire tropics revealed (Randel et al. 2000; Zhou 2000; Zhou et al 2001a, 2001b; Seidel et al. 2001).

4.1. *QBO and ENSO Signatures in the Tropical CPT*

To extract the QBO and ENSO signatures in the tropical CPT, Zhou et al (2001b) used the zonal wind shear at 50 mb (difference between the winds at 40 mb and 70 mb) over Singapore and the sea surface temperature anomaly (SSTA) in the Niño3.4 region as reference indices in the bivariate regression. Mathematically, the SSTA and the QBO are not independent due to the overlap in their frequency domain. A quasi-biennial oscillation in SST has been noted although it is not clear whether it is physically related to the stratospheric QBO (Xu 1992; Meehl 1993; Geller et al. 1997). In order to separate the influences of the stratospheric QBO and the tropospheric ENSO on the tropical CPT, Zhou et al. (2001b) made two independent QBO and SSTA time series using a Butterworth bandpassed filter (Hamming, 1989). The response function of the bandpass filter has the value 1 at a period of 28 months, and ½ at period of about 22 and 34 months. This filter was used to extract the quasi-biennial variabilites from the wind shears at 50 mb over Singapore. For the SSTA, the bandpassed time series was subtracted from the SSTA. The above process can be expressed by the following

$$QBO(t)' = QBO(t)_{22-34m} \qquad (1)$$

$$SSTA(t)' = SSTA(t) - SSTA(t)_{22-34m} \qquad (2)$$

Zhou et al. (2001b) found that the CPT is simultaneously correlated to the ENSO and that the CPT has strongest correlation to the QBO at a time lag. The westerly wind shears at 50 mb

lead warm CPT-T anomalies by about 6 months. Taking this time lag into account, the bivariate regress can be written as follows

$$CPTT(t) = a \times QBO(t-6)' + b \times SSTA(t)' + \gamma(t) \qquad (3)$$

in which *CPTT* is the CPT-T anomalies (subtract the seasonal cycle from the monthly CPT-T) and γ is the residual. Figure 4 shows the composites of CPT-T anomalies associated the QBO, based on regressed time series, i.e. $a \times QBO(t-6)'$, which is adjusted in time. The zonally symmetric features of the QBO in CPT properties are obvious. During the westerly shear period, the composited CPT is warmer by 0.2 to 0.3 K, and during easterly shear conditions it is colder by 0.2 to 0.4 K. There seems to be a stationary wave with wavenumber 2 superposing on a zoanlly homogeneous field. For example, there are minima over the western Pacific and the southern America. However, this asymmetry might be due to the fact that the influence of the QBO and ENSO on the tropical CPT cannot be perfectly separated. Figure 5 shows the composites of the CPT-T anomalies for two El Niños and La Niñas that occurred during 1979-1993 (the two El Nino occurred during April 1982-July 1983 and August 1986-February 1988, and the two La Nina during September 1984-June 1985 and May 1988-January 1989). Generally, the temperature anomalies associated with the ENSO are larger than those associated with the QBO. Figure 5 shows three distinct features. First, there is an east–west (E–W) dipole over the tropical Pacific. The second feature is that there are three north–south (N–S) dumbbells in the Tropics. The strongest dumbbell is over the central to eastern Pacific. One dumbbell pattern is clear over the Atlantic, and similar features are also seen over the eastern Indian Ocean and the western Pacific, though less clearly. The third feature is that there is a maximum (in absolute value) over the equatorial western Pacific. These three features can be explained by changes of tropical convection activity associated with ENSO as will be discussed. Similar features of the CPT variabilities

associated with QBO and ENSO also can be seen in the pressure and height composites (figures not shown), although those features are not as clear as the temperature composites. Similar results were found by Randel et al. (2000) using the NCEP reanalyses and lapse rate tropopause definition.

Geller et al. (2002) used a two-dimensional model to simulate the interannual variability of stratospheric water vapor. They indicated that the QBO modulation of stratospheric water vapor results from two causes. Dynamical redistribution of water vapor from the QBO induced mean meridional circulation dominates the observed variability in the middle and upper stratosphere. In the lower tropical stratosphere, the QBO water vapor variability is dominated by a "tape recorder" that results from the dehydration signal accompanying the QBO variation of the tropical CPT. It is suggested that another low frequency "tape recorder" exists due to ENSO modulation of the tropical CPT.

4.2. *Mechanism for the QBO Signature in the Tropical CPT*

Tropical stratospheric QBO is a significant low-frequency variability and has been intensively investigated for decades (e.g. Reed et al. 1961; Veryard and Ebdon 1961; Plumb and Bell 1982; Naujoket 1986). Zhou et al. (2001b) indicated that the westerly shears at 50mb, which are accompanied by warm temperature anomalies (Plumb and Bell 1982), lead the tropical CPT-T by about 6 months and are positively correlated with the tropical CPT-T. It takes about 3-4 months for the westerly shear at 50mb to reach 100mb and takes about 7 months for the easterly shear to propagate from 50mb to 100mb (Naujoket 1986), which gives an average of about 5-6 months. This time lag is consistent with the analyses by Zhou et al. (2001b). The amplitude of QBO temperature perturbation can be estimated using

$$f_0 \overline{u}_z + H^{-1} R \overline{T}_y = 0 \qquad (4)$$

which is equation (7.1.1d) of Andrews et al. (1987). Given a wind change over a scale height $\Delta\overline{u}$ =10 m/s and a latitudinal scale L=1000 km, eq. (4) gives an estimate of about 0.79 K for temperature change over a distance L. Amplitude of the CPT-T anomalies associated with the QBO is about 0.3-0.5 K (Figure 4). Consistency in time lag and amplitude suggests that the QBO signature in the tropical CPT temperatures is probably due to the stratospheric QBO temperature anomalies that accompany the downward-propagating QBO meridional circulation (Plumb and Bell 1982).

4.3. *Mechanism for the ENSO Signature in the Tropical CPT*

Yulaeva and Wallace (1994) investigated the signature in global temperature and precipitation fields derived from the Microwave Sounding Unit (MSU). The ENSO-associated temperature anomalies in the troposphere (MSU-2) and the lower stratosphere (MSU-4) are consistent with the ENSO signature in the tropical CPT, in respect of the shape and positions of the E–W dipole and N–S dumbbells and the maximum anomaly over the western Pacific. The ENSO has a coherent vertical structure in the tropical atmospheric temperature which reverses sign at certain altitude below the CPT. For instance, during El Niño events, the tropical troposphere (1000-200 mb layer) over the eastern Pacific is warmer and the tropopause and the lower stratosphere is colder. Zhou and Sun (1994) extended the Gill model (Gill 1980) including a cooling over the western domain and a heating over the eastern domain to study the tropical troposphereic nonlinear steady response to two heating sources of contrasting nature. OLR observations indicate positive anomalies (negative diabatic heating anomalies) over the eastern Indian Ocean and the western Pacific and negative anomalies (positive diabatic heating anomalies) over the central to eastern Pacific

(Yulaeva and Wallace 1994). Thus, the distribution of two idealized heat sources considered by Zhou and Sun (1994) represents the longitudinal distribution of major diabatic heating anomlies in the tropics during El Niño events. The steady geopotential height response at the top of model domain to these two heat sources of contrasting nature shows that there is positive dumbbell over the eastern half domain and a negative dumbbell over the western half domain. These positive and negative dumbbells form an E-W (positive-negative) dipole. Additionally, there is a negative maximum geopotential height anomaly to the east of the western cooling source and this maximum anomaly is a result of wave-wave interaction (Zhou and Sun 1994). Thus, the geopotential height response to W-E negative-positive paired heating sources is hydrostically consistent with Figure 5a, which shows the El Niño associated tropical CPT-T anomalies. However, the response of the temperature anomaly was assumed to have the same vertical structure as the heating (Gill 1980; Zhou and Sun 1994). The Gill model needs to be extended further, e.g. including a stratospheric layer or following the framework presented in Highwood and Hoskins (1998), to explain the ENSO signature in the tropical CPT-T more reasonably though results from this model have shown that the E-W dipole feature in the ENSO signature in the tropical CPT is caused by the changes in tropical convection during ENSO events, the N-S dumbbell feature is due to rotation of the earth, and the maximum over the equatorial western Pacific is caused by nonlinear wave-wave interaction (Zhou and Sun 1994).

5. Long-term Trend of the Tropical CPT Temperatures

Zhou et al. (2001a) analyzed the trend of the tropical CPT using tropical daily sounding data. Figure 6 shows tropical monthly mean CPT-T during 1973-1998. A cooling trend (-0.57±0.06 K/Decade during 1973-1998) in the tropical CPT-T can been found. This number

is close to the cooling rate (–0.6K/Decade) found by Simmons et al. (1999) in the global mean 100 mb temperatures. Independent calculation by Seidel et al. (2001) showed a cooling of about –0.5 K/decade at the tropical tropopause. Zhou et al (2001) also calculated the trends for each tropical region and found that the trend of the CPT over the western Pacific is about –0.33±0.08 K/Decade and the trend is a little stronger in other regions.

The trend may be influenced by inhomogeneities in the sounding data. To examine the impact of the inhomogeneity problem, Zhou et al. (2001a) included a few binary terms in the regression equation corresponding to changes in station log, and calculated the trend station by station. It is found that nearly all tropical stations have a cooling trend. The trend is sensitive to the inhomogeneity of the sounding data (Gaffen et al. 2000). However, no statistically significant warming trend has been found.

Zhou et al. (2001a) proposed that the cooling of the tropical tropopause might be caused by changes in tropical convection. If convection occurs more frequently and/or is more intense than in earlier years, then the tropical CPT tropopause will be getting higher and colder. Calculations indicated a warming trend in SST and a negative trend in OLR almost everwhere in the tropics (Waliser and Zhou, 1997). As mentioned above, the tropical tropopause is cooling almost everywhere in the tropics. These three trends are consistent with one another. The warming SST tends to destabilize the static stability of the troposphere, and convection will occur more frequently and/or be more intense. Convective clouds will reach higher altitude or cover a larger area. As an indication of this, the OLR shows a negative trend. Waliser and Zhou (1997) indicated that the negative OLR trend corresponds closely to the positive trend observed directly from the *in situ* rainfall observation. Stronger convection and more precipitation produce larger diabatic heating in the tropics, which forces a higher

tropopause, so the pressures and temperatures of the tropical tropopause become lower and colder.

It is observed that stratospheric water vapor showed a positive trend in the past decades (Rosenlof et al. 2001). There are three factors influencing stratospheric water vapor: methane oxidation, dehydration at the tropical tropopause, and transport by the meridional circulation. The increase in methane emission is too small to explain the observed trend of stratospheric water vapor (Nedoluha et al. 1998). Thus, the cooling trend in the CPT temperatures implies that the positive trend in stratospheric water vapor is probably due to changes in the dynamic circulation. For instance, if more tropospheric air enters the stratosphere through the tropopause in the subtropics where the temperatures are warmer than in the deep Tropics, the water vapor flux into the stratosphere would be larger.

6. Spatial Structure of the "Cold Trap"

In section 2, it was pointed that a paradox exists about the western Pacific. Air moving from the troposphere into the stratosphere needs to be dehydrated in this region, but the wind analysis indicated a downward motion tin the region. To solve this paradox, Holton and Gettelman (2001) proposed a mechanism model in which the zonally moving air encounters the "cold trap" in response to radiative cooling of subvisible cirrus lying above deep convective anvil clouds. According to this mechanism, the three-dimensional structure of the "cold trap" and its variations are important.

Figure 7 shows vertical section of 15-year mean temperature in January and July over the equator, which was based on ECMWF reanalysis monthly temperature field. Cubic spline fitting was applied to obtain temperatures near the tropopause. It can be seen that the "cold trap" is about 4 K colder in winter than in summer, and 0.5 km higher in winter. The

horizontal section of the temperature filed at a given altitude near the tropopause, e.g. 17 km in winter, looks like Figure 1. The saturation water vapor mixing ratio near the tropopause strongly depends on the temperature, and slightly depends on the pressure. If we define the "cold trap" to be the volume enclosed the surface 190 K, one can conceive the general structure of the wintertime "cold trap" combining Figure 1a and Figure 7a. In Figures 1a and 7a, values below 192 K instead of 190 K were shaded since the ECMWF reanalysis overestimates the tropopause temperatures by about 2 K. The height of the "cold trap" is about 1.5 km. The upwelling velocity in the tropical lower stratosphere is about 0.2~0.4 mm/s (Plumb and Eluszkiewicz 1999). It takes about 2 months for an air parcel to climb 1.5 km in the tropical lower stratosphere. During this period, the air parcel travel about 1.3 rounds along the equator, assuming a zonal wind speed of 10 m/s. Thus, most air parcels, which enter the stratosphere at regions other than the western Pacific, have a chance to encounter the "cold trap" and get dehydrated. Air parcels, which enter the stratosphere about one month earlier, also can encounter the "cold trap".

Animation of monthly mean temperatures reveals complicated interannual variations of the "cold trap". Daily fields show even complicated features. It is important to investigate what causes variations of the "cold trap" and how variations of the "cold trap" determine the concentration of stratospheric water vapor.

7. Summary

Much progress about the tropical tropopause has been made in recent years. It includes progress in studies of seasonal cycle, intraseasonal variations, interannual variations, and long term trend of the tropical tropopause. It seems tropical convection plays important role in tropopause variations. For the timescale of a few hours, Teitelbaum et al. (2000) found an

almost simultaneous response of the tropical CPT to strong convection in limited observations. For the intraseasonal time scale, the CPT temperature anomalies in the deep Tropics leads the OLR anomalies by about one quarter major period, and are likely the Kelvin wave excited by convection that occurs to their west (Zhou and Holton 2002). The annual cycle of the tropopause is mainly driven by the extratropical stratospheric wave forcing (Yulaeva et al. 1994), but the zonal asymmetry of the tropical tropopause is attributed to the asymmetry of the distribution of tropical convection (Highwood and Hoskins, 1998). At interannual timescales, the tropical tropoppause is affected by the QBO and the ENSO. The signature of the QBO in the tropopause is mainly zonally symmetric, but the ENSO signature shows dipole and dumbbell patterns (Zhou 2000; Randel et al. 2000; Zhou et al. 2001a). These patterns are believed to be stationary Rossby and Kelvin waves associated with tropical convection (Zhou et al. 2001b). Zhou et al. (2001a) found a cooling trend in the tropical CPT and this trend is consistent with trends in tropical SST, OLR and *in situ* precipitation. It was suggested that the trend in the tropical tropopause is caused by changes in tropical convection.

The general picture of STE is clear. Tropospheric air enters the stratosphere across the tropical tropopause where it is dehydrated by the cold temperature. The air was transported to high altitudes and high latitudes by the residual circulation, while methane oxidation increases water vapor concentration. Finally, it returns to the troposphere at polar region, where polar stratospheric air experiences a second dehydration due to the cold temperature inside the polar vortex. However, our knowledge about STE is far from complete. Many uncertainties mainly lies in the tropical tropopause region. For simplicity, tropical tropopause is often treated as if it were a surface without thickness. In fact, the tropopause is better thought of as a transition layer (Highwood and Hoskins 1998; Sherwood and Dessler 2001).

Studies about the transition layer tropopause is very limited due to its complexity. However, understanding the structure and variations of the "cold trap" and many processes (sedimentation and/or re-evaporation of ice crystals, cooling by overshooting convective turrets etc.) in the transition layer is crucial for studies on STE.

Acknowledgments

References

Andrews, D. G., J. R. Holton, and C. B. Leovy, 1987: Middle atmospheric dynamics, Academic Press.

Atticks, M. and G. Robinson, 1983: Some features of the structure of the tropical tropopause, *Quart. J. Roy. Meteor. Soc.,***109**, 295-308.

Boehm, M. T. and J. Verlinde, 2000: Stratospheric influence on upper tropospheric tropical cirrus, *Geophys. Res. Lett*, **27**, 3209-3212.

Brewer, A. M., 1949: Evidence for a world circulation provided by the measurements of helium and water vapor distribution in the stratosphere, *Quart. J. Roy. Meteor. Soc.,* **75**, 351-363.

Dobson, G. M. B., 1956: Origin and distribution of polyatomic molecules in the atmosphere, *Pro. R. Soc. London, Ser.* **A236**, 187-193.

Dunkerton, T. J., 1978: On the mean meridional mass motions of the stratosphere and mesosphere, *J. Atmos. Sci.*, **35**, 2325-2333.

Frederick, J. E. and A. R. Douglass, 1983: Atmospheric temperatures near the tropical tropopause: Temporal variations, zonal asymmetry and implications for stratospheric water vapor, *Mon. Wea. Rev.*, **111**, 1397-1401.

Gaffen, D. J., M. A. Sargent, R. E. Habermann, and J. R. Lanzante, 2000: Sensitivity of the tropospheric and stratospheric temperature trends to radiosonde data quality, *J. Climate*, **13**, 1776-1796.

Gage, K. S. and G. C. Reid, 1987: Longitudinal variations in tropical tropopause properties in relation to tropical convection and ENSO events, *J. Geophys. Res*., **92**, 14 197-14 203.

Geller, M. A., W. Shen, M. Zhang, and W. Tan, 1997: Calculation of the stratospheric quasi-biennial oscillation for time-varying forcing, *J. Atmos. Sci.*, **54**, 883-894.

Geller, M. A., X.-L. Zhou and M. Zhang, 2002: Simulations of the interannual variability of stratospheric water vapor, *J. Atmos. Sci.*, **59**, 1076-1085.

Gettelman, A., A. R. Douglass, and J. R. Holton, 2000: Simulations of water vapor in the upper troposphere and lower stratosphere, *J. Geophys. Res*., **105**, 8317-9003-9023.

Gill, A. E., 1980: Some simple solutions for heat induced tropical circulation, *Quart. J. Roy. Meteor. Soc*., **106**, 447-462.

Hamming, R. W., 1989: Digital filter, Prentice-Hall, Inc., 3rd ed. p284.

Heddon, H. H. and M. L. Salby, 1994: The life cycle of the Madden-Jullian oscillation, *J. Atmos. Sci*., **51**, 2225-2237.

Heddon, H. H. and M. L. Salby, 1996: Planetary-scale circulations forced by intraseasonal variations of observed convection, *J. Atmos. Sci.,* **53**, 1751-1758.

Highwood, E. J. and B. J. Hoskins, 1998: The tropical tropopause, *Quart. J. Roy. Meteor. Soc.*, **124**, 1579-1604.

Holton, J. R., and A. Gettelman, 2001: Horizontal transport and the dehydration of the stratosphere, *Geophy. Res. Lett.,* **28,** 2799-2802.

Holton, J. R., M. J. Alexander, and M. T. Boehm, 2001: Evidence for short vertical wavelength Kelvin waves in the DOE-ARM Nauru99 radiosonde data, *J. Geophys. Res*., **106**, 20 125-20 129.

Kiladis, G. N., K. H. Straub, G. C. Reid, and K. S. Gage, 2001: Aspects of interannual intraseasonal variability of the tropopause and lower stratosphere, *Quart. J. Roy. Meteor. Soc.*, **127**, 1961-1984.

LeTexier, H. S., H. S. Solomon, and R. R. Garcia, 1988: The role of molecular hydrogen and methane oxidation in water vapor budget of the stratosphere, *Quart. J. Roy. Meteor. Soc*., **114**, 281-295.

Madden, R. A. and P. R. Jullian, 1994: Observations of the 40-50 day tropical oscillation — A review, *Mon. Wea. Rev*., **122**, 814-837.

Meehl, G. A., 1993: A coupled air-sea biennial mechanism in the tropical Indian and Pacific regions: role of the ocean, *J. Climate*, **6**, 31-40.

Mote, P. W., K. H. Rossenlof, M. E. McIntyre, E. S. Carr, J. C. Gille, J. R. Holton, J. S. Kinnersley, H. C. Pumphrey, J. M. Russell III, and J. W. Waters, 1996: An atmospheric tape recorder: the imprint of tropical tropopause temperatures on stratospheric water vapor, *J. Geophys. Res*., **101**, 3989-4006.

Nedoluha, G. E., R. M. Bevilacqua, R. M. Gomez, D. E. Siskind, B. C. Hicks, J. M. Russell III, and B. J. Conner, 1998: Increases in middle atmospheric water vaporobserved by the Halogen Occultation Experiment and the ground-based water vapor millimeter-wave spectrometer from 1991-1997, *J. Geophys. Res.*, **103**, 3531-3543.

Newell, R. E. and S. Gould-Stewart, 1981: A stratospheric fountain, *J. Atmos. Sci*., **38**, 2789-2795.

Plumb, R. A. and R. C. Bell, 1982: Equatorial waves in steady zonal shear flow, *Quart. J. Roy. Meteor. Soc.*, **108**, 313-334.

Plumb, R. A. and J. Eluszkiewicz, 1999: The Brewer-Dobson circulation: dynamics of the tropical upwelling, *J. Atmos. Sci*., **56**, 868-890.

Randel, W. J., F. Wu, and D. J. Gaffen, 2000: Interannual variability of the tropical tropopause derived from radiosonde data and NCEP reanalyses, *J. Geophys. Res*., **105**, 15 509-15 523.

Reid, G. C. and K. S. Gage, 1981: On the annual variation in eight of the tropical tropopause, *J. Atmos. Sci.*, **38**, 1928-1938.

Reid, G. C. and K. S. Gage, 1985: Interannual variation in the height of the tropical tropopause, *J. Geophys. Res*., **90**, 5629-5635.

Reid, G. C. and K. S. Gage, 1996: The tropical tropopause over the western Pacific: wave driving, convection and the annual cycle, *J. Geophys. Res*., **101**, 21 233-21 242.

Rosenlof K. H., S. J. Oltmans, D. Kley, J. M. Russell III, E.-W. Chiou, W. P. Chu, D. G. Johnson, K. K. Kelley, H. A. Michelsen, G. E. Nedoluha, E. E. Remsberg, G. C. Toon, M. P. McCormick, 2001: Stratospheric water vapor increases over the past half-century, *Geophy. Res. Lett.*, **28**, 1195-1198.

Seidel, D. J., R. J. Ross, J. K. Angell, and G. C. Reid, 2001: Climatological characteristics of the tropical tropopause as revealed by radiosondes, *J. Geophys. Res*., **106**, 7857-7878.

Simmons, A. J., A. Untch, C. Jakob, P. Kallberg, and P. Unden, 1999: Stratospheric water vapor and tropical tropopause temperatures in ECMWF reanalyses and multi-year simulations, *Quart. J. Roy. Meteor. Soc.,* **125**, 353-386.

Sherwood, S. C., 2000: A stratospheric "drain" over the maritime continent, *Geophys. Res. Lett*., **27**, 677-680.

Sherwood, S. C., and A. E. Dessler, 2001: A model for transport across the tropical tropopause, *J. Atmos. Sci.*, **58**, 765-779.

Teitelbaum, H., M. Moustaoui, C. Basdevant, J. R. Holton, 2000: An alternative mechanism explaining the hygropause formation in tropical region, *Geophys. Res. Lett*, **27**, 221-224.

Vicent, D. G., A. Fink, J. M. Schrage, and P. Speth, 1998: High and low-frequency intraseasonal variations of OLR on annual and ENSO timescales, *J. Climate*, **11**, 968-986.

Wheeler, M., G. N. Kiladis, and P. J. Webster, 2000: Large-scale dynamical fields associated with convectively coupled equatorial waves, *J. Atmos. Sci.*, **57**, 613-640.

Xu, J. S. 1992: On the relationship between the stratospheric quasi-biennial oscillation and the tropospheric southern oscillation, *J. Atmos. Sci.*, **49**, 725-734.

Yulaeva, E., J. R. Holton, and J. M. Wallace, 1994: On the cause of annual cycle in the tropical lower stratospheric temperature, *J. Atmos. Sci*., **51**, 169-174.

Yulaeva, E. and J. M. Wallace, 1994: The signature of ENSO in global temperature and precipitation fields derived from the microwave sounding unit, *J. Climate*, **7**, 1719-1736.

Zhou, X.-L., 2000: The tropical cold point tropopause and stratospheric water vapor, Ph.D dissertation, State University of New York, 121 pp.

Zhou, X.-L. and Z. Sun, 1994: Tropical atmospheric nonlinear steady response solution under effects of paired heat sources of contrasting nature, *ACTA Meteor. Sin*., **8**, 356-364.

Zhou, X.-L., M. A. Geller and M. Zhang, 2001a: The cooling trend in the tropical cold point tropopause temperatures and its implications, *J. Geophys. Res*., **106**, 1511-1522.

Zhou, X.-L., M. A. Geller and M. Zhang, 2001b: Tropical cold point tropopause characteristics derived from ECMWF reanalyses and sounding, *J. Climate*, **14**, 1823-1838.

Zhou, X.-L. and J. R. Holton, 2002: Intraseasonal variations of tropical cold point tropopause temperatures, *J. Climate*, **15**, 1460-1473.

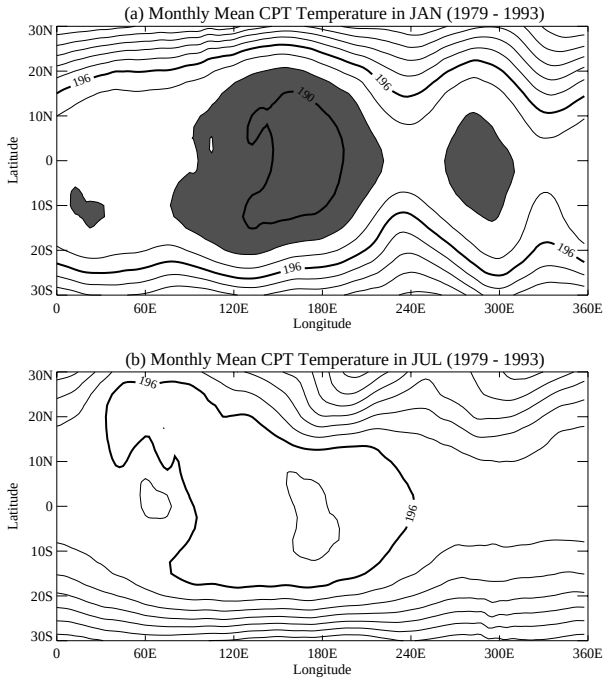

Figure 1: Monthly mean CPT temperature (a: January; b: July) averaged over the ECMWF reanalyses period (1979-1993). The contour interval is 2 K. Areas with values below 192 K are shaded. Note that an overestimate of about 2 K in ECMWF-based CPT-T calculations was not deducted (Zhou et al., 2001a).

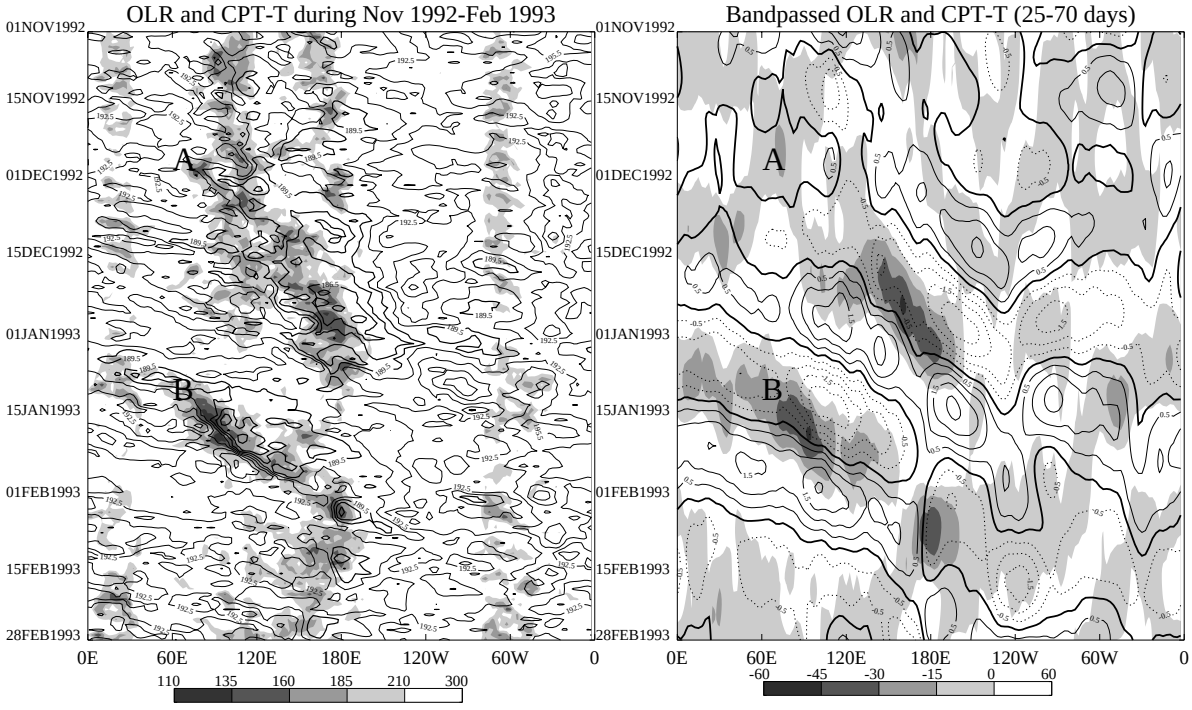

(a) Unfiltered

(b) Bandpassed

Figure 2: Time-longitude sections of (a) unfiltered (left) and (b) 25-70 day band-passed (right) OLR (shaded) and CPT-T (contoured) averaged over the latitude band 5°S-5°N. Shading scale for OLR (Wm^{-2}) is indicated by the bar at the bottom. The contour interval for CPT-T is 1.5 K in the left column, and 0.5 K in the right column. Contours less than 190 K are indicated by thick curves In the left column (Zhou and Holton 2002).

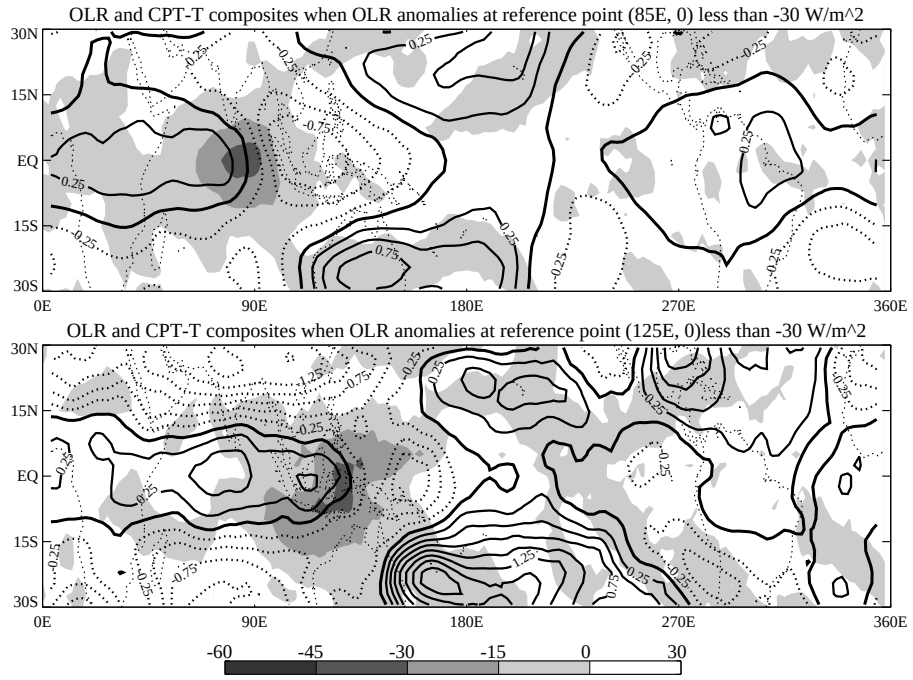

Figure 3: Composites of 25-70 day bandpassed OLR (shaded) and CPT-T (contoured) anomalies during the period when the 25-70 day bandpassed OLR at reference points (top) (0°, 85°E) and (bottom) (0°, 85°E) are less than -30 Wm^{-2}. The shading scale for OLR anomalies is indicated by the bar at the bottom. Contour interval for the CPT-T composites is 0.25 K (Zhou and Holton 2002).

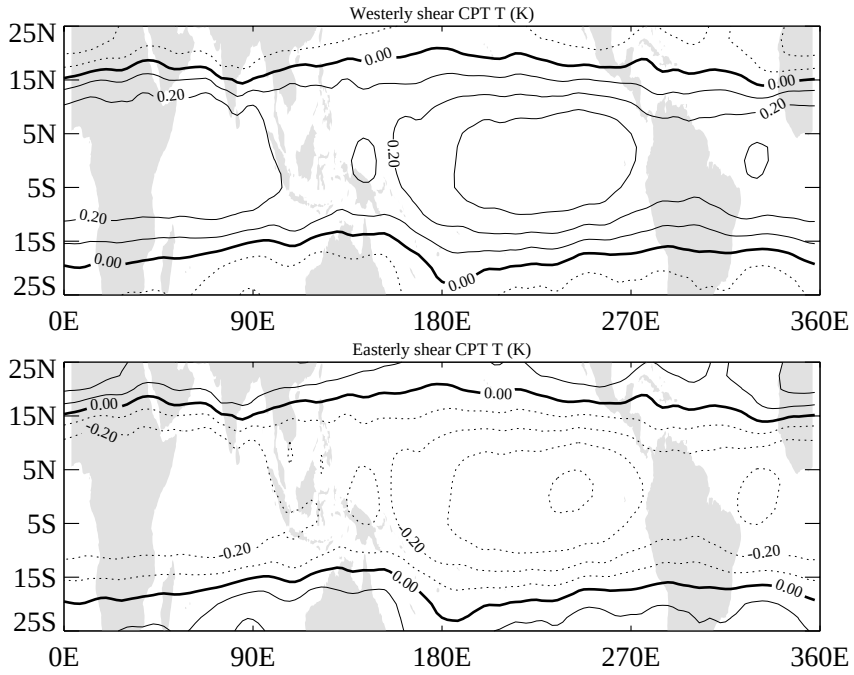

Figure 4: Composite analysis of CPT-T under westerly (upper) and easterly (lower) stratospheric zonal wind shear conditions. Note that the shears lead the CPT-T by 6 months. Contour interval is 0.1 K (Zhou et al. 2001b).

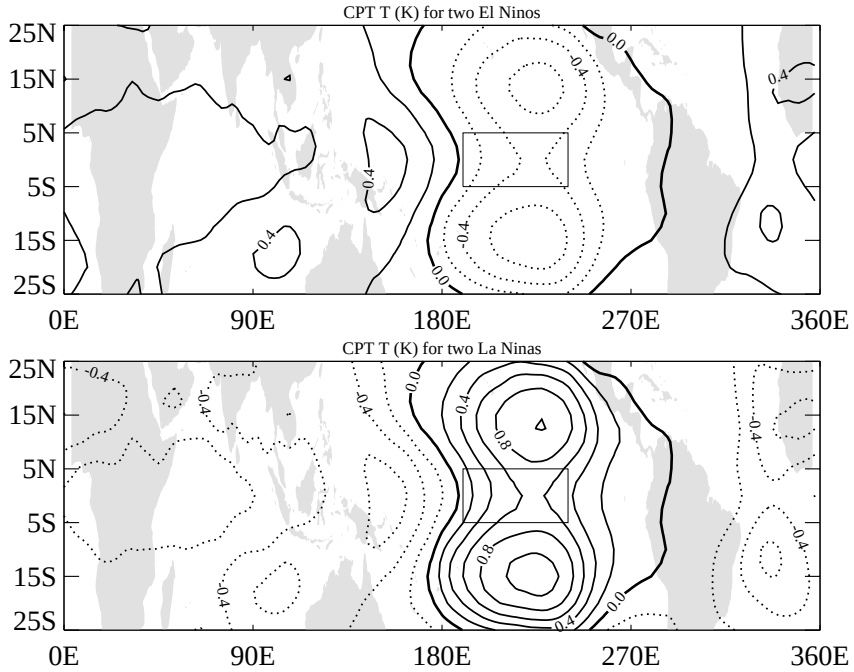

Figure 5: Composite analysis of CPT-T during two ENSO events that occurred during 1979-1993. See the text for the selection of ENSO events. Square boxes show the Niño3.4 region. COntour interval is 0.2 K (Zhou et al. 2001b).

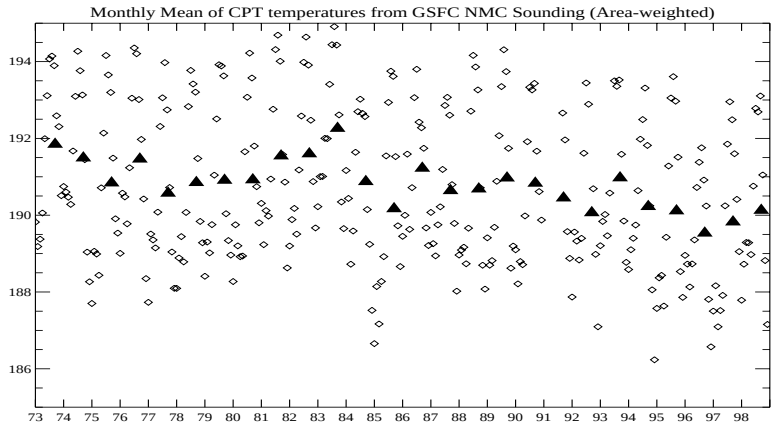

Figure 6: Monthly mean temperatures over the entire tropical cold point tropopause (CPT) in 1973-1998 calculated from operational sounding profiles (diamonds) and their annual means (triangles). Temperature is in Kelvin (Zhou et al. 2001a).

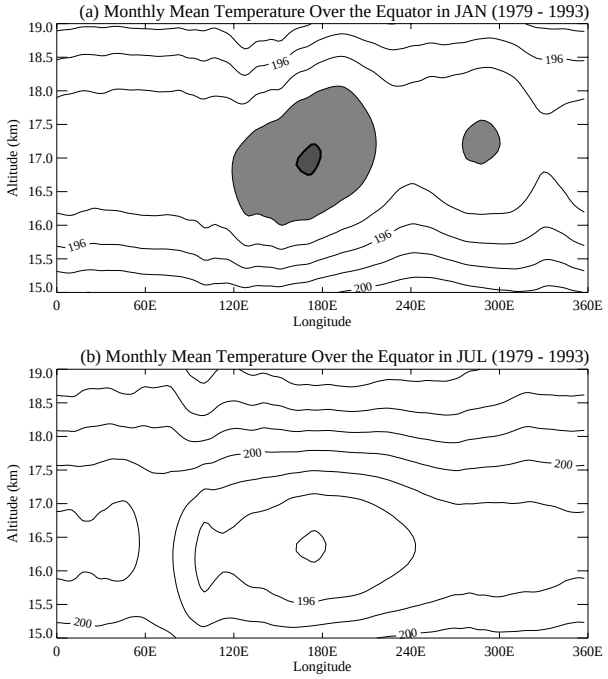

Figure 7: Vertical sections of monthly mean temperature near the tropical tropopause (a: January; b: July) averaged over the ECMWF reanalyses period (1979-1993). The contour interval is 2 K. Areas with values below 192 K are shaded.